

Electronic Spectra of Jet-Cooled Anthracene Dimer: Evidence of Two Isomers in the Electronic Ground State

Tomohiro Matsuoka, Kentaro Kosugi,[†] Kazuyuki Hino, Masaharu Nishiguchi, Kazuhiko Ohashi, Nobuyuki Nishi,[†] and Hiroshi Sekiya*

Department of Chemistry, Faculty of Science, Kyushu University, Hakozaki 6-1, Higashi-ku, Fukuoka 812-8581, Japan

Received: March 17, 1998; In Final Form: July 9, 1998

The broad and sharp absorption systems of anthracene in the 362–376 nm region have been confirmed to be due to dimeric species by measuring the resonantly enhanced two-photon ionization mass spectrum. The hole-burning spectrum indicated that two stable isomers exist in the S_0 state. The decay time of the excimer emission (300 ns) from the broad system is much longer than that of the emission from the sharp system (15 ± 5 ns), indicating that the electronic nature of the excited state is very different between the two systems. The difference in the excited-state potentials of the two systems has been discussed on the basis of the vibronic structures and the emission lifetimes.

1. Introduction

The study of the electronic spectra of the aromatic van der Waals (vdW) clusters has been of considerable interest in excited-state dynamics such as intramolecular vibrational redistribution, charge transfer, and excimer formation. However, little is known about the structures of aromatic vdW clusters even in the electronic ground state. The most extensively studied system is the benzene dimer, for which “T-shape” geometry in the electronic ground state has been confirmed.^{1–7} The size and excess energy dependence of excimer formation in naphthalene clusters was studied in detail.⁸ The excimers of anthracene clusters^{9–13} and the exciplexes of anthracene with various adducts^{14–17} have been studied to investigate exciton and charge-transfer interactions.

Anthracene dimers were observed in hydrocarbon matrices,^{9–11} in a helium jet,¹² and in LB films.¹³ Recently, Chakraborty and Lim¹² observed two absorption systems in the 365–376 nm region of the fluorescence excitation spectrum of jet-cooled anthracene. One system is very broad and structureless with an intensity maximum at 367.8 nm, whereas a structured absorption system with sharp peaks was observed in the region of 372–376 nm. The excitation of the two absorption systems provided strongly red-shifted emission. The two systems were tentatively assigned to “T-shaped” and “stacked (parallel displaced)” dimers, respectively.¹² The assignment of dimeric species was made by measuring the temperature dependence of the absorption intensity, and the size of the species was not confirmed. In addition, no direct evidence has been obtained for the existence of the two isomers. To discuss the structure and the excited-state dynamics of the anthracene dimer(s), more detailed characterization of the spectrum such as vibrational assignments and the fluorescence decay times as well as the confirmation of the cluster size is necessary.

In this work, we have presented more detailed results on the two absorption systems of anthracene. It has been confirmed

that the broad and sharp absorption systems are due to dimeric species by measuring the resonantly enhanced two-photon ionization (R2PI) mass spectrum. The nanosecond time-resolved spectrum and the hole-burning spectrum have been successfully applied to distinguish the two absorption systems. The hole-burning spectrum unambiguously indicates that two stable isomers exist in the S_0 state. Dual fluorescence has been observed from the broad system. The decay time of a long component of the broad system is much longer (300 ns) than the corresponding decay time of the sharp system (15 ns). The difference in the excited-state potentials of the two systems has been discussed by comparing the vibronic structures and the emission lifetimes.

2. Experimental Section

Zone-refined anthracene was purchased from Wako Pure Chemical Industries Ltd., and was used without further purification. The vacuum chamber was evacuated by a 10-in. diffusion pump backed by a 1200 L/min oil rotary pump.¹⁸ The nozzle housing was heated to 100–200 °C with a coiled heater to obtain sufficient vapor pressure for the measurement of the excitation spectrum of the anthracene vdW complexes. The vaporized anthracene mixed with helium was expanded into the vacuum chamber with a pulsed nozzle (General valve $D = 0.5$ mm). The backing pressure of He (P_0) was 1–5 atm. The vdW complexes produced in a free jet were probed with a XeCl excimer laser pumped dye laser (Lumonics EX600 and HD300). The pulse width of the dye laser was 8 ns. Fluorescence was detected with a photomultiplier (Hamamatsu 1P28A). The photocurrent signal was averaged with a 500-MHz digital storage scope (LeCroy 9400). Nanosecond time-resolved fluorescence was measured by setting a time window on the storage scope. Dispersed fluorescence spectra were measured by using a $f = 0.25$ m monochromator (Nikon 6250). Time-resolved dispersed fluorescence spectra were measured in the same manner the measurement of the fluorescence excitation spectrum. For the measurement of the hole-burning spectrum, the frequency doubled output of the idler light of an OPO system (Spectra Physics GCR-200 and MOPO-730) was used for the

* To whom correspondence should be addressed.

[†] Present address: Institute for Molecular Science, Myodaiji, Okazaki 444-8585, Japan.

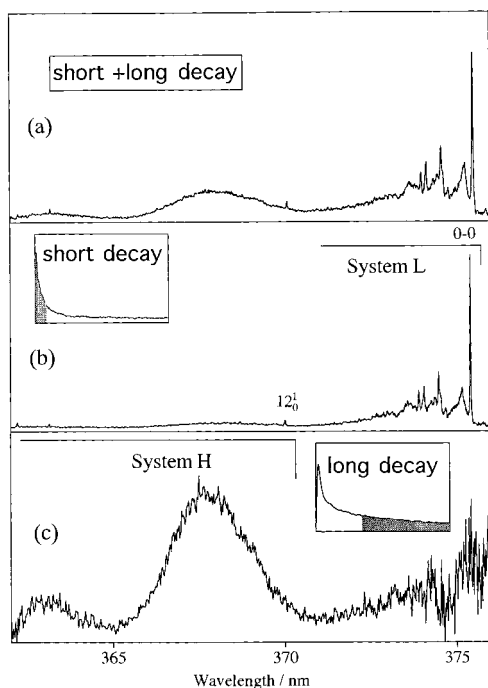


Figure 1. Time-resolved fluorescence excitation spectra of anthracene clusters measured by monitoring at wavelengths longer than 510 nm with a sharp cutoff filter (Toshiba Y-51). The experimental conditions were $P_0 = 5.0$ atm and $X/D = 20$, and the nozzle temperature was 180 °C. The inserted figures schematically indicate the fluorescence decay profiles obtained from the excitation of system L for (b) and system H for (c). The widths of the time window are indicated by the shadow. Spectra (a)–(c) were measured by adjusting the time window to cover the short and long, short, and long decays, respectively.

probe laser, while the output of the dye laser system (Lumonics HE700 and HD300) was employed for the pump laser. The two beams propagated coaxially along light baffles mounted on the side of the vacuum chamber to reduce stray light. The beam of the probe laser was unfocused, while that of the pump laser was mildly focused. A typical delay time between the pump and probe lasers was 300 ns. The fluorescence-dip signal was detected with a photomultiplier and averaged with a storage scope while the wavelength of the probe laser was scanned.

The mass spectrum of anthracene clusters was measured by using a two-color R2PI technique with use of a reflectron-type mass spectrometer.¹⁹ The intensity of the ion current detected with the dual microchannel plate was too weak to measure the R2PI spectrum.

3. Results

Excitation Spectrum and Fluorescence Decay Time. Two absorption systems with broad and sharp band features are observed in the regions of 365–371 and 371–376 nm, respectively, in Figure 1a. The spectrum was obtained by monitoring fluorescence at wavelengths longer than 510 nm with a cutoff filter. When we monitored the emission at a wavelength longer than 420 nm, no significant change in the vibronic pattern was observed. We refer to the two absorption systems in the high-energy region of 365–371 nm and the low-energy region of 371–376 nm as H and L, respectively. The intensity ratio of the two systems H to L was almost constant for the variation of the sample temperature (nozzle temperature) in the range of 140–200 °C, suggesting that the two systems H and L originate from the same size of anthracene cluster. The intensity ratio H to L and the intensity distribution within the sharp features are

TABLE 1: Fluorescence Excitation Spectrum of Anthracene Dimer in the Region of 370–376 nm

wavenumber	$\Delta\nu$	intensity ^a	assignment
26660.5	−30.5	vw	hot band
26630.0	0	vs	0–0
26647.8	17.8	s	im ^b
26681.8	51.8	w	im
26695.4	65.4	s	im
26703.7	73.7	w	im
26712.9	82.9	w	im
26726.3	96.3	s	im
26737.3	107.3	s	im
27020.1	390.0	vw	12 ₀ ¹

^a The abbreviations vs, s, w, and vw indicate very strong, strong, weak, and very weak bands, respectively. ^b im indicates intermolecular vibration.

somewhat different from those in the spectrum of Chakraborty and Lim.¹² The intensity of the most intense peak at 375.4 nm relative to the sidebands in Figure 1a is much stronger than that reported,¹² while that of system H is relatively weaker than that of system L in Figure 1a. These differences may be due to saturation of the absorption in the previous spectrum.¹² We measured the excitation spectrum by varying the dye laser power. The spectra in Figure 1 were measured with a low laser power, while the spectrum obtained with a high power became more similar to the spectrum in the literature.¹² We have assigned the strongest peak at 375.4 nm ($\nu = 26630.0$ cm^{−1}) to the electronic origin band of system L. When the excitation spectrum was observed under the warmer conditions, a very weak hot band appeared red-shifted by 30.5 cm^{−1} from the origin band. The band positions and relative frequencies of sharp peaks are listed in Table 1. Most of low-frequency bands with frequencies 18–108 cm^{−1} may be due to intermolecular vibrational modes, since such low-frequency modes have not been observed in the spectrum of the anthracene monomer.²⁰ An anthracene dimer has six intermolecular modes composed of three translational and three rotational combinations. We noted that the frequency of a sharp peak at 0–0 + 390 cm^{−1} is very similar to that of the ν_{12} mode of the monomer (389 cm^{−1}) in the S₁ state,²⁰ which appears prominently in the absorption spectrum, indicating that system L is unambiguously originating from the complex involving anthracene and not due to an unknown impurity. A much weaker intensity of the ν_{12} mode of the complex than that of the monomer may be due to a very fast nonradiative process from the vibronic level. This prediction is consistent with the intensity distribution of vibronic bands in the hole-burning spectrum which will be described in the following section.

Typical fluorescence decay profiles following the excitation at the maximum of system H (367.8 nm) and the origin band of L (375.4 nm) are shown in Figure 2a,b, respectively. It should be noted that two decay profiles are very different. A very long decay component is involved in the decay profile of H, while the decay time of L is short. The fluorescence decay time of system L was fitted to a single-exponential function followed by the deconvolution of the instrumental response function and determined to be 15 ± 5 ns. The magnitude of the decay time was independent of the wavelength monitored. The fluorescence intensity of system H was very weak, and it was difficult to remove the scattered laser light. The profile in Figure 2a was obtained by subtracting the contribution of the scattered light. Therefore, the experimental deviation of the short lifetime was estimated to be as large as 5 ns. The decay time of the longer component was measured to be 330 ± 20 ns from the slope of log plots of the intensity. The decay time of

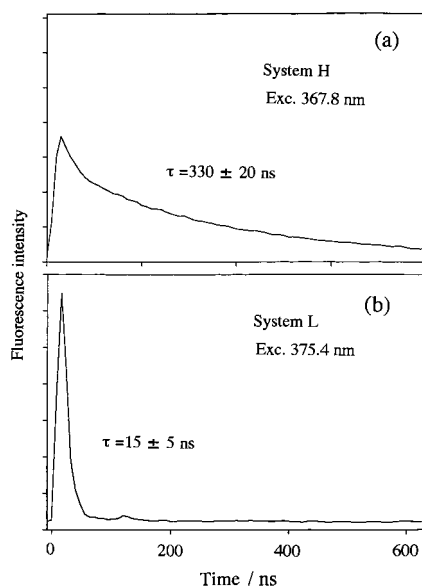


Figure 2. Fluorescence decay profiles measured by exciting (a) the band at 367.8 nm and monitoring the wavelength at 400–500 nm by using band-pass filters (Toshiba G-50 and C-39A) and (b) the band at 375.4 nm and monitoring at 430 nm with a monochromator (15 Å bandwidth). The contribution of the intensity of the scattered laser light was large for a and very small for (b). The contribution of the scattered light was subtracted from the observed decay profiles. A small peak at 120 ns in (b) is due to noise. The decay time τ in (a) was obtained from the profile in the time region longer than 100 ns (see the text).

L is shorter than that of the monomer (25 ± 5 ns) measured by exciting the 0–0 band, but that of H is much longer.

We have measured the nanosecond time-resolved fluorescence excitation spectrum by varying the width of the time window. The excitation spectra measured by adjusting the time window to the short and long decays are shown in Figure 1b,c, respectively. It is clear that the short-decay component is predominant for system L, whereas the long-decay component is much stronger for system H, from a comparison of the three spectra in Figure 1. We noted that the spectral feature of system H does not depend on the position of the time window, suggesting that system H is originating from only one species. A broad feature is observed in Figure 1b in the region of 372–376 nm. The intensity of this feature increased with the temperature of the sample, indicating that the absorption of a larger cluster is overlapping with that of the dimer. Thus, the measurement of the time-resolved spectra unambiguously indicates that two different absorption systems H and L exist.

Hole-Burning Spectrum. Figure 3b shows the hole-burning spectrum measured by probing the 0–0 transition of system L. A progression of the ν_{12} mode is clearly observed in this spectrum. A lot of low-frequency bands are built on the ν_{12} mode. The vibronic structure in the region of 374–375.5 nm is similar to that in the fluorescence excitation spectrum (Figure 3a). However, low-frequency vibronic bands disappeared in the fluorescence excitation spectrum. The low-frequency bands must be due to intermolecular modes. The increase in the vibrational state density may enhance the nonradiative process toward higher vibrational excitation energy than 200 cm^{-1} of the zero-point level in the upper state of system L. It is difficult to conclude whether absorption system H is observed or not in Figure 3c, because the absorption intensity of system H is about one order smaller than that of the origin band of system L and the sensitivity of the hole-burning spectrum is too low to discriminate a weak broad absorption. However, system L as well as system H is not observed in Figure 3c, obtained by

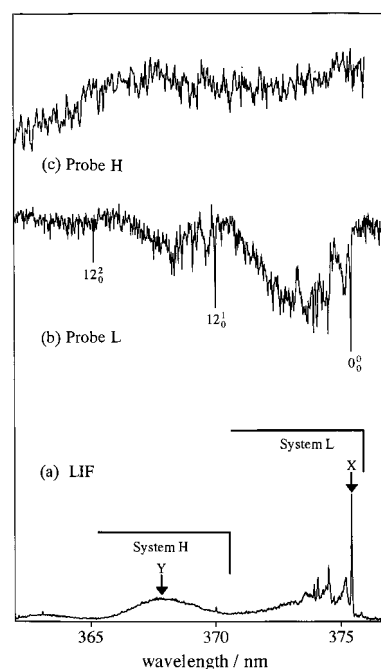


Figure 3. Fluorescence excitation (a) and hole-burning spectra (b) and (c) of anthracene dimer. Spectra b and c were measured by probing the 0–0 transition of system L and the intensity maximum (367.8 nm) of system H, respectively. The wavelength of the probe laser is indicated by the arrow. The decrease in the intensity below 365 nm was not reproducible and was due to the change in the intensity of the probe laser.

probing the intensity maximum at 367.8 nm. The absence of system L in Figure 3c indicates that the electronic ground state of system H is not identical to that of system L.

Very recently, we have observed the hole-burning spectrum as well as the fluorescence excitation and dispersed fluorescence spectra of 2-methylanthracene dimer.²¹ Two absorption systems of the 2-methylanthracene dimer corresponding to H and L of anthracene were separately observed in the hole-burning spectrum, indicating that two isomers exist in the S_0 state. This result is consistent with the observation of the two isomers for anthracene dimer.

Mass Spectrum. The observation of the R2PI spectrum may provide conclusive evidence for the size of the clusters. To confirm the cluster size, we have measured the mass spectrum by using the R2PI technique, because the ion current was too weak to obtain the R2PI spectrum. The wavelength of the ionization laser was 275.1 nm, while that of the probe laser was varied around the S_1 – S_0 region of the bare anthracene. The ion current was detected by the reflectron mass spectrometer.¹⁹ Two peaks due to a dimer and the monomer were observed for the excitation into the 362–370 nm region. The monomer peak was mainly due to the dissociation after one-color, two-photon ionization of the dimer species. In addition to the dimer peak, a peak of trimer is observed for the excitation of the wavelength region of 372–376 nm. The observed mass spectra suggested that the absorption of dimer ranges from 363 to 376 nm, while that of trimer exists in the region longer than 372 nm. The cluster size determined by the mass spectrum is consistent with the result from the fluorescence excitation spectrum; e.g., the intensity ratio of the two systems L and H was almost constant for the variation of the temperature of the sample. However, the combination of the results of the mass spectrum with the fluorescence excitation spectrum provided more detailed information on the excitation spectrum; the absorption system of a trimer exists as a background in the

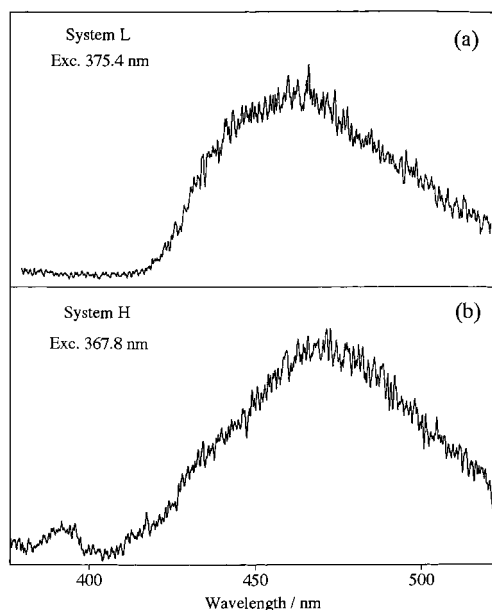


Figure 4. Dispersed fluorescence spectra obtained by exciting into (a) 375.42 nm of system L and (b) 367.8 nm of system H, respectively. The time window was adjusted to cover the time range of both the short and long decays.

fluorescence excitation spectrum of system L in the wavelength longer than 372 nm.

Dispersed Fluorescence Spectrum of Anthracene Dimer.

The dispersed fluorescence spectrum in Figure 4a was measured by exciting the band at 375.4 nm (system L) and adjusting the time window to the short decay, while Figure 4b was obtained by exciting the band at 367.8 nm (system H) and the time window was adjusted to cover the time range of both the short and long decays. In the region of 420–520 nm a very broad feature with a maximum at 465 nm is observed in Figure 4a, while a much broader feature is observed in the wavelength region larger than 410 nm with a maximum at 470 nm in Figure 4b. It should be noted that a prominent band is observed at 392 nm in Figure 4b in addition to the weak broad emission, whereas no corresponding band is observed in Figure 3a. A weak broad band was detected in the region around 410 nm in the dispersed fluorescence spectrum measured by exciting the band at 375.44 nm (system L) by Chakraborty and Lim.¹² They ascribed this band to large clusters. An anthracene trimer which was observed in our mass spectrum as well as the dimer might be excited in the spectrum of Chakraborty and Lim.¹² The absence of the corresponding band in Figure 4 indicates that the concentration of the trimer is much lower in our experimental conditions.

To investigate the band at 392 nm in Figure 4b, we have measured the time-resolved dispersed fluorescence spectra by exciting the band at 367.8 nm (system H) and changing the width and the position of the time window. Parts a–c of Figures 5 were obtained by monitoring the short and long decays, short decay, and long decay, respectively. The position and the width of the time window are illustrated in each inserted figure, which was obtained by exciting the band at 367.8 nm. It is clear that the weak band at 392 nm in the dispersed fluorescence spectrum is originating from a short decay. The decay time of this short component was roughly estimated to be much less than 100 ns from the measurement of the intensity of the band at 392 nm while varying the width of the time window. Thus both short and long decays exist for the emission from H; the former decay

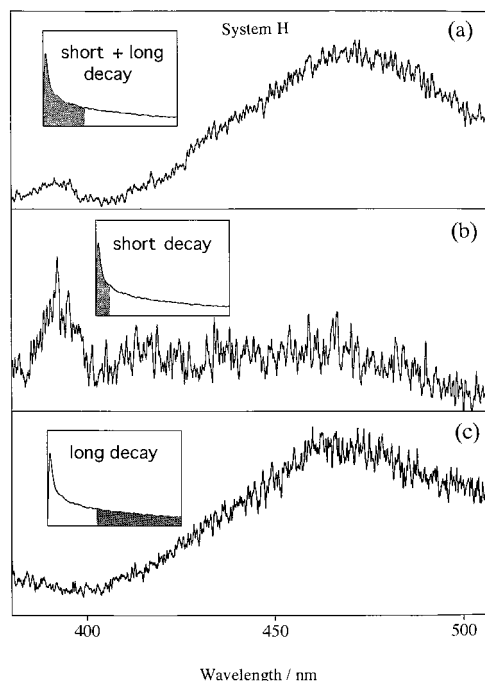


Figure 5. Time-resolved dispersed fluorescence spectra of dimer H measured by varying the time window. The inserted figures indicate the fluorescence decay profile measured upon the excitation at 367.8 nm with monitoring at wavelengths longer than 510 nm. The shadow schematically indicates the width and the position of the time window.

may be due to the resonance emission while the latter one to excimer emission.

4. Discussion

The measurement of the R2PI mass spectrum confirmed that the two systems H and L are due to dimeric species of anthracene. The photoexcitation at the H band provides dual emission, whereas the L system excitation provides only the red-shifted emission. Dual emission was not observed by the excitation of system H in previous work of Chakraborty and Lim.¹² The observation of dual emission from the excited states of H is consistent with short and very long (300 ± 20 ns) decays. The former and the latter decays may be due to the resonance fluorescence and to the emission from a different dimer conformation, respectively. The latter is the dominant decay process when system H is excited. In contrast, the excitation of system L provides only red-shifted broad emission with a short decay time (15 ± 5 ns).

Significant differences exist in the vibronic pattern of the spectra and the spectral shifts from the monomer between systems H and L. The spectral feature of system L is similar to that in the excitation spectrum of the fluorene dimer, in which the electronic origin and several low-frequency vibronic bands were observed.²¹ The exciton splitting has not been identified in the spectrum of L. No regularity has been found in the intervals between the intermolecular vibrational frequencies. We have newly observed a broad feature in the region of 361–365 nm for system H in addition to the broad band at 367.8 nm. The interval between the maxima of the two broad bands is about 360 cm^{-1} . Therefore, we have assigned the bands at 367.8 and 363.0 nm to the 0–0 and 12_0^1 transitions, respectively.

On the basis of the above experimental findings we can obtain qualitative information about the change in the geometry of the dimer and the excited-state potentials. System L must be due to the excitation into the locally excited (LE) state, and the

change in the geometrical structure upon photoexcitation may be rather small as judged from the sharp structured vibronic pattern. The short decay is thought to be due to the excimer formation. The transformation from the LE state to the excimer state must be very fast. Such very fast transformation of the LE state to the excimer state has been suggested in the fluorene,²² 9-ethylfluorene,²³ and naphthalene^{8,24} dimers.

The excited-state potential energy surface for system H could be inferred on the basis of the broad spectral feature and unusual long decay time of the excited state. A similar broad feature was observed in the fluorescence excitation spectrum of the dibenzofuran dimer^{25,26} and was ascribed in part to the coupling between the LE state and the lower excimer state and in part due to low-frequency intermolecular vibrational structure.²⁶ Chakraborty and Lim²⁵ considered that, at energies lower than the 0–0 band of the S_1 – S_0 absorption, the optical transition from the ground-state van der Waals dimer directly prepares the excimer state (E^*) of dibenzofuran, from which the broad structureless excimer fluorescence originates. At energies corresponding to the S_1 – S_0 absorption of the dimer, photoexcitation of the vdW dimer leads to the appearance of dual emission, which is composed of the structured S_1 – S_0 fluorescence and unstructured E^* – S_0 excimer fluorescence. A similar strong coupling of the LE state to the excimer state observed in the dibenzofuran dimer²⁵ may exist in the anthracene dimer. The photoexcitation of the ground-state dimer may directly prepare the E^* state, leading to both the broad E^* – S_0 excimer emission and sharp resonance emission. Thus, we can consistently explain the dual emission as well as the broad spectral features of system H by considering the directly prepared excimer state.

We noted that a close similarity exists between the excitation spectra of systems L and H of the anthracene dimer and those of the 1:1 anthracene–dimethylaniline complex measured by Brenner et al.¹⁷ in the 360–370 nm region. The hole-burning spectra indicated that two structural isomers exist for the anthracene–dimethylaniline complex. An isomer provides a lot of sharp low-frequency bands built on the ν_{12} mode, whereas two broad peaks separated by 385 cm^{-1} were observed in the spectrum of the other isomer. The difference in the two absorption systems was interpreted by the strength of the A^*D – A^-D^+ coupling, where D and A are electron donor and acceptor, respectively. The excitation of the A–D system prepares state A, which has both the A^*D and A^-D^+ character. In the weak coupling case, the potential surface of the A state is almost identical to that of the locally excited state or ion state. In the strong coupling case, a strong mixing of sparse LE and dense ion state occurs. The oscillator strength of the LE vibrational levels is redistributed to among a large number of mixed levels. In view of the high-level density, the individual transitions in absorption overlap so that the absorption band becomes broad and structureless. The charge-resonance (CR) interaction was suggested to be important for the formation of excimer/exciple by Yip and Levy²⁶ and Murrel and Tanaka.²⁷ In the present work no exciton resonance has been observed, and we infer that strong coupling between the LE and CR states may exist in the excited electronic state of system H as is the case for the anthracene–dimethylaniline exciple.¹⁷

A question is, why the decay time of the excimer emission from H (300 ns) is much longer than the lifetimes of the excimer emission from fluorene (70 ns) and 9-ethylfluorene (98 ns).²³ The emission lifetimes of the jet-cooled exciplexes of anthracene and substituted anthracenes with various adducts^{14–17} are helpful in understanding the long decay times of H. Very long decay

times were observed upon excitation of some broad absorption bands of the 1:1 anthracene–dimethylamine (220 ns)¹⁴ and anthracene–ammonia complexes ($450 \pm 100\text{ ns}$)¹⁵ and the 1:2 2-methylanthracene–diethyl ether (470 ns) complex.¹⁶ The long decay times are explained by a weak overlap of the ground- and excited-state electronic wave function of the exciple. The results of the anthracene exciplexes may suggest that the long decay time of the emission from system H is associated with an ionic character of the excimer state.

5. Conclusion

Two sharp and broad absorption systems of anthracene in the 362–376 nm region have been ascribed to the transitions from the S_0 states of isomers of dimeric species by measuring the time-resolved spectrum, mass spectrum, and hole-burning spectrum. The excitation of the broad system provides both the resonance and excimer emission, while only the excimer emission was observed by exciting the sharp system. The sharp and broad features of the spectra are interpreted as being due to the difference in the coupling of the LE state with the CR state. The coupling is weak in the sharp system, while very strong coupling may exist in the excited electronic state of the broad system. The decay times of the excimer emission are very different for the photoexcitation of the two systems, indicating that the electronic nature in the excited state is very different. A strong charge-transfer character may be responsible for the long decay time of the excimer emission from the broad system.

Acknowledgment. The authors thank Dr. H. Sakashita at the Center of Advanced Instrumental Analysis, Kyushu University, for allowing us to use a Nikon monochromator.

References and Notes

- (1) Janda, K. C.; Heminger, J. C.; Winn, J. S.; Novick, S. E.; Harris, S. J.; Klemperer, W. J. *J. Chem. Phys.* **1975**, *63*, 1419.
- (2) Steed, J. M.; Dixon, T. A.; Klemperer, W. J. *J. Chem. Phys.* **1979**, *70*, 4940.
- (3) Law, K. S.; Schauer, M.; Bernstein, E. R. *J. Chem. Phys.* **1984**, *81*, 4871.
- (4) Bornsen, K.; Selzle, H. L.; Schlag, E. W. *J. Chem. Phys.* **1986**, *85*, 1726.
- (5) Henson, B. F.; Hartland, G. V.; Venturo, V. A.; Felker, P. M. *J. Chem. Phys.* **1992**, *97*, 2189.
- (6) Hobza, P.; Selzle, H. L.; Schlag, E. W. *J. Phys. Chem.* **1993**, *97*, 3937.
- (7) Arunan, E.; Gutowski, H. S. *J. Chem. Phys.* **1993**, *98*, 4294.
- (8) Saigusa, H.; Lim, E. C. *J. Phys. Chem.* **1995**, *99*, 15738, and references cited therein.
- (9) Ferguson, J. *J. Chem. Phys.* **1966**, *44*, 2677.
- (10) Chandross, E. A.; Ferguson, J.; MacRae, E. G. *J. Chem. Phys.* **1966**, *45*, 3546.
- (11) Ferguson, J.; Mau, A. W.-H.; Morris, J. *Aust. J. Chem.* **1974**, *27*, 713.
- (12) Chakraborty, T.; Lim, E. C. *J. Phys. Chem.* **1993**, *97*, 11151.
- (13) Mukai, I.; Akimoto, S.; Ito, T.; Ohta, T.; Yamazaki, I. *Chem. Lett.* **1997**, 263.
- (14) Anner, O.; Haas, Y. *Chem. Phys. Lett.* **1985**, *119*, 199.
- (15) Anner, O.; Haas, Y. *J. Phys. Chem.* **1986**, *90*, 4298.
- (16) Anner, O.; Haas, Y. *J. Am. Chem. Soc.* **1988**, *110*, 1416.
- (17) Brenner, V.; Millie, Ph.; Piuze, F.; Tramer, A. *J. Chem. Soc., Faraday Trans.* **1997**, *93*, 3277.
- (18) Sekiya, H.; Nagashima, Y.; Nishimura, Y. *J. Chem. Phys.* **1990**, *92*, 5761.
- (19) Ohashi, K.; Nishi, N. *J. Chem. Phys.* **1993**, *98*, 390.
- (20) Peng, L. W.; Keelan, B. W.; Semmes, D. H.; Zewail, A. H. *J. Phys. Chem.* **1988**, *92*, 5540, and references cited therein.
- (21) Hino, K.; Sekiya, H. Unpublished results.
- (22) Saigusa, H.; Itoh, M. *J. Phys. Chem.* **1985**, *89*, 5486.
- (23) Itoh, M.; Morita, Y. *J. Phys. Chem.* **1988**, *92*, 5693.
- (24) Saigusa, H.; Sun, H.; Lim, E. C. *J. Phys. Chem.* **1992**, *96*, 2083.
- (25) Chakraborty, T.; Lim, E. C. *Chem. Phys. Lett.* **1993**, *207*, 99.
- (26) Yip, W. T.; Levy, D. H. *J. Phys. Chem.* **1996**, *100*, 11539.
- (27) Murrel, J. N.; Tanaka, J. *Mol. Phys.* **1964**, *7*, 363.